



## ■ KNEE

# The effects of posterior cruciate ligament deficiency on posterolateral corner structures under gait- and squat-loading conditions

A COMPUTATIONAL KNEE MODEL

**K-T. Kang,  
Y-G. Koh,  
M. Jung,  
J-H. Nam,  
J. Son,  
Y.H. Lee,  
S-J. Kim,  
S-H. Kim**

Yonsei University,  
Seoul, South Korea

■ K-T. Kang, PhD, Researcher, Department of Mechanical Engineering,  
■ J-H. Nam, MS, Researcher, Department of Mechanical Engineering,  
■ J. Son, MS, Researcher, Department of Mechanical Engineering, Yonsei University, 50 Yonsei-ro, Seodaemun-gu, Seoul, 03722, South Korea.  
■ Y-G. Koh, MD, Orthopaedic surgeon, Joint Reconstruction Center,  
■ S-J. Kim, MD, Orthopaedic surgeon, Joint Reconstruction Center, Department of Orthopaedic Surgery, Yonsei Sarang Hospital, 10 Hyoryeong-ro, Seocho-gu, Seoul, 06698, South Korea.  
■ M. Jung, PhD, Researcher, AnyBody Technology A/S, 10 Niels Jernes Vej, Aalborg, 9220, Denmark.  
■ Y. H. Lee, MD, Associate professor, Department of Radiology, Yonsei University College of Medicine, 50-1 Yonsei-ro, Seodaemun-gu, Seoul, 03722, South Korea.  
■ S-H. Kim, MD, Assistant professor, Department of Orthopedic Surgery, Yonsei University College of Medicine, Gangnam Severance Hospital, 211 Eonju-ro, Gangnam-gu, Seoul, 06273, South Korea.

Correspondence should be sent to S-H. Kim; email: orthohwanbm@gmail.com

doi: 10.1302/2046-3758.61.  
BJR-2016-0184.R1

*Bone Joint Res* 2017;6:31–42.  
Received: 7 June 2016;  
Accepted: 6 November 2016

## Objectives

The aim of the current study was to analyse the effects of posterior cruciate ligament (PCL) deficiency on forces of the posterolateral corner structure and on tibiofemoral (TF) and patellofemoral (PF) contact force under dynamic-loading conditions.

## Methods

A subject-specific knee model was validated using a passive flexion experiment, electromyography data, muscle activation, and previous experimental studies. The simulation was performed on the musculoskeletal models with and without PCL deficiency using a novel force-dependent kinematics method under gait- and squat-loading conditions, followed by probabilistic analysis for material uncertain to be considered.

## Results

Comparison of predicted passive flexion, posterior drawer kinematics and muscle activation with experimental measurements showed good agreement. Forces of the posterolateral corner structure, and TF and PF contact forces increased with PCL deficiency under gait- and squat-loading conditions. The rate of increase in PF contact force was the greatest during the squat-loading condition. The TF contact forces increased on both medial and lateral compartments during gait-loading conditions. However, during the squat-loading condition, the medial TF contact force tended to increase, while the lateral TF contact forces decreased. The posterolateral corner structure, which showed the greatest increase in force with deficiency of PCL under both gait- and squat-loading conditions, was the popliteus tendon (PT).

## Conclusion

PCL deficiency is a factor affecting the variability of force on the PT in dynamic-loading conditions, and it could lead to degeneration of the PF joint.

Cite this article: *Bone Joint Res* 2017;6:31–42.

**Keywords:** Knee biomechanics, Knee injury, Posterior cruciate ligament

## Article focus

■ This study considered the predicted kinematics and muscle activation of the knee in a dynamic situation and assessed the biomechanical effect of posterior cruciate ligament (PCL) deficiency on posterolateral corner structures and joint contact forces of the knee.

## Key messages

■ The popliteal tendon was the most important posterolateral structure in

regards to the condition of PCL deficiency.

■ Degeneration of the patellofemoral joint could be caused by high flexion dynamic activity.

## Strengths and limitations

■ Strength: this study validated a novel biomechanical methodology applied to the condition of the dynamic knee, particularly the posterolateral corner, which has rarely been studied

- Limitation: Analysis of a single subject may not represent the general clinical situation considering anatomical variation, gender-, and age-related changes, which could be complementary by additional larger scale experiments.

## Introduction

The posterior cruciate ligament (PCL) is a fundamental stabiliser of the knee joint, but its biomechanical mechanism has not been fully understood or investigated.<sup>1-3</sup> The reported incidence of acute PCL injuries ranges from 1% to 44% of acute knee injuries.<sup>4</sup> Isolated PCL injuries are less common than those with other concomitant ligamentous conditions.<sup>5,6</sup> The most frequent type of injury associated with PCL injury is that of the posterolateral corner structure, leading to posterolateral rotatory instability. The approach for treating PCL injuries remains a controversial issue in sports medicine. The majority of clinicians have reported treating PCL injuries without any operative interventions.<sup>7-9</sup> Medial-sided injuries, in particular, can be conservatively healed using non-operative treatment methods. In contrast, lateral-sided and injuries to the posterolateral corner structure require, and have been more successfully treated with, surgical repair and/or reconstruction.<sup>10-12</sup>

Posterolateral corner structure, the injury of which often accompanies that of PCL, contains the lateral collateral ligament (LCL), popliteus tendon (PT), and popliteofibular ligament (PFL). LCL and PFL are the primary static stabilisers of posterolateral corner structures, and PT is a dynamic stabiliser of the knee joint. Another issue associated with PCL injury is the long-term progress of degenerative changes in the tibiofemoral (TF) and patellofemoral (PF) joints.<sup>13,14</sup> In a previous study that included 38 patients with a mean follow-up of 13.4 years post PCL injury, eight patients underwent surgery for a meniscal tear, and radiographic examinations revealed that the rate of articular cartilage degeneration increased.<sup>15</sup>

In order to understand better the mechanism underlying PCL deficiency, several biomechanical research studies have evaluated the force exerted on posterolateral corner structures and contact forces on TF and PF joints. In previous studies, the force exerted on the PCL with selective cutting of posterolateral corner structure was evaluated.<sup>16-19</sup> Most of these studies were experimental and used cadavers in quasi-static conditions, or *in vivo* studies using dual fluoroscopy.<sup>16-23</sup> To the best of our knowledge, there have been no studies that have investigated the biomechanical effects of PCL deficiency on contact forces in the TF and PF joints, and on forces exerted on posterolateral corner structures under dynamic-loading conditions.

The method for *in vitro* dynamic studies involve laboratory experiments using cadavers in a physiological gait simulator, along with finite element analysis (FEA) and multibody dynamic (MBD) simulation.<sup>24-26</sup> Moreover,

the majority of FEA studies do not include a physiological model associated with anatomical information of bone and muscles.<sup>27</sup> Recently, dynamic computational analysis tools, including musculoskeletal (MSK) MBD structures, have been introduced. These technologies allow dynamic simulations and three-dimensional MSK modelling beyond statistical analyses. MSK models provide a practical alternative to dynamic simulation with elastic ligament bundles that represent the overall kinematic behaviour of the joint.<sup>28,29</sup>

The aim of the present study was to develop a validated subject-specific MSK lower extremity model that allows for 12-degree-of-freedom (DOF) motion at both the TF and PF joints. First, to validate the subject-specific MSK model, values were evaluated and compared with passive flexion results transformed electromyography (EMG) measurements for the subjects' knee joints, including an assessment of the propagation of uncertain ligament properties using probabilistic simulation, under gait- and squat-loading conditions. In addition, the posterior drawer test result in intact and PCL deficiency conditions were compared with previous experiments. Second, the contact forces exerted on the TF and PF joints were evaluated to investigate cartilage degeneration and posterolateral corner structure forces in order to establish the biomechanical effects of PCL deficiency in gait- and squat-loading conditions, including an assessment of the propagation of uncertain ligament properties using probabilistic simulation.

We hypothesised that validated dynamic mechanics improves MSK simulation. We also hypothesised that the PT is the most important component of the posterolateral corner structure in the PCL deficiency condition as a dynamic stabiliser under dynamic loading conditions.

## Patients and Methods

**Passive flexion and EMG experiments.** This study was approved by the hospital's Institutional Review Board. Subject-specific data were used for MSK model development with validations using CT data in passive flexion and motion-capture with EMG sensors.

The subject of this study was a 36-year-old man (178 cm, 75 kg). Radiological findings showed that his knee was normal, without any history of MSK system diseases, or related diseases. The knee was examined with a 0.6 mm slice thickness using a 64-channel CT scanner (SOMATOM Sensation 64, Siemens Healthcare, Erlangen, Germany) with respect to six flexion angles (15°, 30°, 45°, 60°, 75°, 90°) of the knee joint. CT images had been taken for six months to protect the subject from radiation based on the radiation dose reduction protocol that minimised hazardous exposure. In each scan, CTDIvol was 11.48 mGy which is the same radiation dose in routine protocol.<sup>30-32</sup> The tube parameters were 120 kVp and 135 mA, and the acquisition matrix was 512 × 512; the field of view was 200 mm.

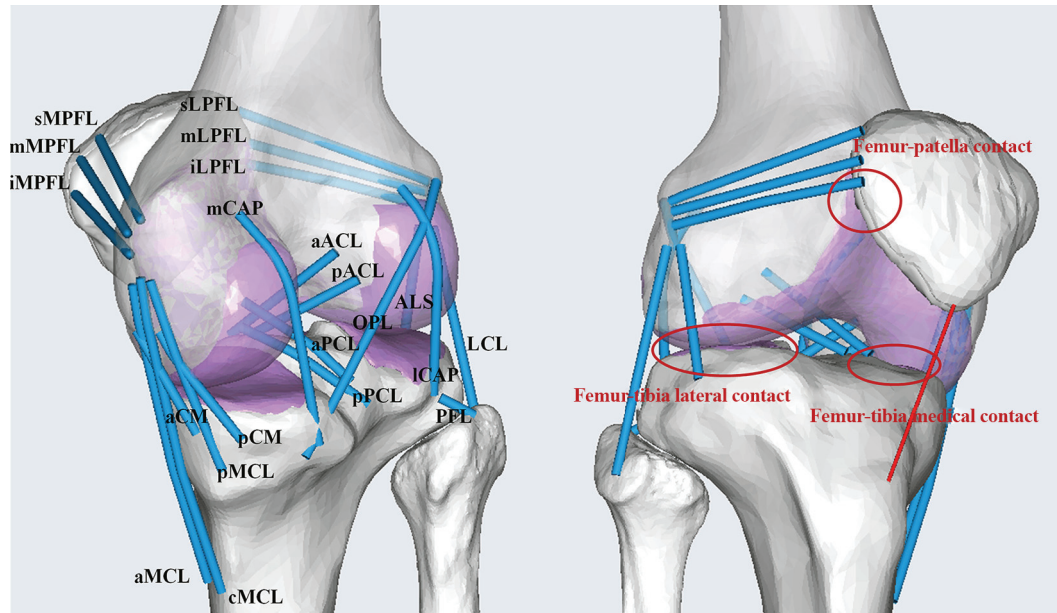


Fig. 1

Schematic of the knee model with contact conditions and 21 ligament bundle: The aACL and pACL; aPCL and pPCL; anterolateral structures; LCL; popliteofibular ligament PFL; medial collateral ligament (aMCL, cMCL, and pMCL); deep medial collateral ligament (aCM and pCM); medial and lateral posterior capsules (mCAP and ICAP, respectively); oblique popliteal ligament; medial patellofemoral ligament (sMPFL, mMPFL, and iMPFL); and lateral patellofemoral ligament (sLPFL, mLPFL, and iLPFL).

Knee joint kinematics were measured based on a previous methodology and included the joint coordinate system during passive flexion testing.<sup>33</sup> Passive flexion data were used in validation of the MSK model. The subject performed four trials of gait- and squat-loading activities, and ground reaction forces were measured using a force plate. The subjects' ground reaction forces were measured using two force plates (800 mm × 600 mm, AMTI, Niles, Illinois). A motion-capture system (Vicon MX, Oxford Metrics, United Kingdom) consisting of 11 infra-red video cameras collected marker trajectories at a sampling rate of 250 Hz. An eight-channel surface EMG system (Bagnoli System, Delsys Inc., Boston, Massachusetts) was used to record EMG signals. Eight EMG signals, marker trajectories, and analogue force plate data associated with gait- and squat-loading conditions were used in this study. The measured muscles included the gluteus maximus, rectus femoris, vastus lateralis, biceps femoris, semi-membranosus, gastrocnemius medialis, tibialis anterior, and soleus medialis. Raw data from the EMG signals were transformed into muscle activation data using root mean square analysis. EMG-to-activation model was used to represent the underlying muscle activation dynamics. The specification of EMG-to-activation transformation has been reported in a previous study.<sup>34</sup>

**Subject-specific MSK model.** A three-dimensional MSK model of the subject-specific knee joint was developed using the AnyBody Modeling System (version 6.0.6; AnyBody Technology, Aalborg, Denmark). To simplify the development process of an entirely subject-specific model, the lower extremity MSK model was extracted

from the AnyBody Managed Model Repository (version 1.6.4) and modified for this study.<sup>35</sup>

The lower extremity MSK model was developed from the Twente Lower Extremity Model anthropometric database.<sup>36</sup> The MSK model was actuated by approximately 160 muscle units. This model has been validated by previous studies to predict muscle and joint reaction forces during locomotion.<sup>37,38</sup> The three-dimensional reconstruction and development procedures for a subject-specific model have been reported by previous studies.<sup>39-41</sup> The ligament insertion points were referenced to the anatomy from the subject's MRI.

Based on the subject's three-dimensional femoral, tibial, fibular, and patellar models, the scales of bone in AnyBody were adjusted using the non-linear radial basis functions with a law of scaling. The remaining parts were adjusted with the scale using an optimisation scheme that minimises the difference between model markers and identified marker positions. In this study, the knee joint was considered to have 12-DOF movement (TF: 6-DOF, PF:6-DOF). Hip and ankle joints were considered to provide 2- and 3-DOF movement, respectively.

The ligament attachment sites were obtained from the subject's MRI image. The attachment points in the AnyBody model were modified using the subject-specific attachment sites. As shown in Figure 1, 21 ligament bundles were modelled. The abbreviation of ligament bundles are shown in Table I. These were modeled in AnyBody using non-linear spring elements with the piecewise force-displacement relationship based on their functional bundles at the actual ligament anatomy.<sup>42</sup>

**Table 1.** Abbreviations for the names of ligament bundle

Abbreviation	Name	Abbreviation	Name
aACL	anterior cruciate ligament	aPCL	posterior cruciate ligament
pACL	anterior cruciate ligament	pPCL	posterior cruciate ligament
aCM	deep medial collateral ligament	mCAP	posterior capsule
pCM	deep medial collateral ligament	ICAP	posterior capsule
sMPFL	medial patellofemoral ligament	sLPFL	lateral patellofemoral ligament
mMPFL	medial patellofemoral ligament	mLPFL	lateral patellofemoral ligament
iMPFL	medial patellofemoral ligament	iLPFL	lateral patellofemoral ligament
aMCL	medial collateral ligament	LCL	lateral collateral ligament
cMCL	medial collateral ligament	ALS	anterolateral structures
pMCL	medial collateral ligament	PFL	popliteofibular ligament
OPL	oblique popliteal ligament		

The stiffness-force relationship of the ligaments in this model is defined so as to produce a nonlinear elastic characteristic with a slack region.<sup>42</sup>

$$f(\varepsilon) = \begin{cases} \frac{k\varepsilon^2}{4\varepsilon_1}, & 0 \leq \varepsilon \leq \varepsilon_1 \\ k(\varepsilon - \varepsilon_1), & \varepsilon > 2\varepsilon_1 \\ 0, & \varepsilon < 0 \end{cases}$$

$$\varepsilon = \frac{l - l_0}{l_0}$$

$$l_0 = \frac{l_r}{\varepsilon_r + 1}$$

Regarding the formulae, the character  $f(\varepsilon)$  is the current force,  $k$  is the stiffness,  $\varepsilon$  is the strain, and  $\varepsilon_1$  is assumed to be constant at 0.03. The ligament bundle slack length,  $l_0$ , can be calculated from the reference bundle length,  $l_r$ , and the reference strain,  $\varepsilon_r$ , in the upright reference position.

Most of the stiffness and reference strain values were obtained from the literature, but some of them have been modified.<sup>42-44</sup> The menisci were modelled by linear springs to simulate their equivalent resistance.<sup>45</sup> The wrapping surface using a cylinder and an ellipsoid was applied in order to prevent ligament penetration on the bone. Furthermore,<sup>1-3</sup> wrapping surfaces were applied to each ligament to wrap the bony structure around the tibia, femur, and patella.

Figure 2 shows three different contact surfaces defined in the TF and PF joints. Three deformable contact models were defined between the femoral and tibial components and between the femoral component and patellar button. These contact forces are proportional to the penetration volume and the so-called 'Pressure Module'.<sup>44</sup> The contact Pressure Module in Newtons per meter cube is the key parameter in the default force-dependent kinematics computational framework of AnyBody.<sup>46</sup> Because the contact model implemented in AnyBody very closely

followed the elastic foundation theory, the equations were derived by Fregly et al.<sup>35,46</sup> For the pressure module calculation, the equation derived by Fregly et al.<sup>46</sup> was used.

**Popliteus muscle modification.** The PT in posterolateral corner structures from AnyBody was modified to minimise the effects of inaccuracy (Fig. 2) in order to represent a more realistic anatomy.<sup>47,48</sup> The default popliteus muscle, composed of two bundles, was modified to represent a third bundle. The origin was modified to be located on each different anatomical position as identified via MRI. The PFL was modified so that it was connected with the popliteus muscle.

**Inverse dynamic simulation and loading conditions.** Before performing inverse dynamic analyses, the kinematics of each trial were calculated on the basis of motion-capture data; kinematic optimisation was used for this purpose. Experimental ground reaction forces and marker trajectories were imported into the AnyBody MSK modelling system in order to calculate muscle forces based on the muscle recruitment criterion (cubic polynomial used in this study) for inverse dynamic analysis. The objective of optimisation was to minimise the difference between the AnyBody model marker trajectories and the motion-capture marker trajectories. After kinematic optimisation was completed, muscle force was evaluated through inverse dynamic analysis. Muscle activation and ligament force were calculated using inverse dynamic analysis, and muscle activations were compared with EMG signals.

To evaluate the effect of uncertainty in ligament stiffness and reference strains on knee kinematics under passive flexion, Monte Carlo (MC) simulations (1000 trials) were performed. The Isight (Simulia, Providence, Rhode Island) Simcode was used with AnyBody to run the MC simulations. A passive flexion test condition, from full extension to 90° of flexion, was applied. The standard deviation of the linear stiffness was 30% of the ligament stiffness and 0.02 of the reference strain.<sup>49</sup> Gait and squat simulations were performed with a subject-specific MSK model, which was validated using a passive flexion test



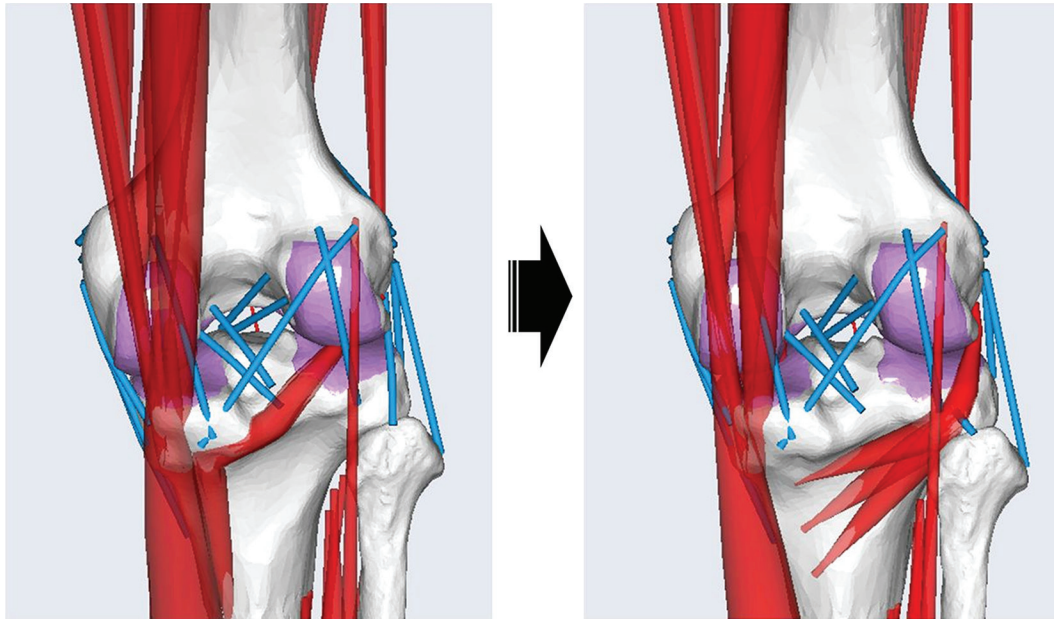


Fig. 2

Schematic of the popliteus muscle modification.

performed on the subject, and used to predict muscle activation (Fig. 3). The posterior tibial translations in the posterior drawer test under intact and PCL deficiency conditions with 134 N at 30° and 90° of flexion were compared with previous experimental studies.<sup>50-54</sup> In order to understand the influence of PCL deficiency, the increase in ligament forces on the PFL, LCL, and PT were evaluated. In addition, the contact forces on the TF and the PF were evaluated. MC simulations were performed in order to consider uncertainty caused by differences of individual's material properties of ligaments. The result of PCL deficiency was represented by the predicted mean value.

## Results

**Comparison of passive flexion, posterior drawer and EMG experimental results with a computational model.** Measurements of TF kinematics using flexion CT for passive flexion–extension movements showed consistency with model predictions, generally lying within the uncertainty range in simulation (Fig. 4). TF translations and internal tibial rotation are the most sensitive factors that influence a ligament's properties. The greatest muscle activities evaluated from the computational model showed consistency with transformed EMG measurements under gait- and squat-loading conditions (Fig. 5). However, there was a different trend due to an increase in the prediction error for the tibial anterior muscle.

In the posterior drawer test at 134 N, the intact posterior tibial translations were 5.2 mm and 4.0 mm at 30° and 90° of knee flexion, respectively, while those in the PCL deficiency condition were 10.3 mm and 12.3 mm at 30° and 90° of knee flexion, respectively (Fig. 6). For both the intact and PCL-deficient knee joint, the variations in

translation were within the ranges as demonstrated in previous experimental studies.<sup>50-54</sup>

**Posterolateral corner ligament force and knee joint contact force under gait- and squat-loading conditions.** The graphs in Figure 7 show the probability analysis and forces on PFL, LCL, and PT with PCL deficiency in the gait- and squat-loading condition. The mean ligament forces on the PFL, LCL, and PT increased by 5%, 19%, and 21%, respectively, with PCL deficiency in the gait-loading condition (Fig. 7a). The mean ligament force on the PFL was not significantly influenced by PCL deficiency in the gait-loading condition.

The graphs in Figure 8 show the probability analysis and contact forces on the TF and PF joints with PCL deficiency in the gait- and squat-loading condition. The mean TF contact force was 1.7 times body weight or 1360 N, and the mean PF contact force was 1.3 times body weight, or 1060 N, with an intact model in the gait-loading condition (Fig. 8a). The contact forces on lateral and medial TF joints were 0.86 and 1.7 times body weight, respectively, with an intact model in the gait-loading condition. The contact force on the medial side was greater than that on the lateral side, with an intact model in the gait-loading condition. A similar trend was observed in the model with PCL deficiency. The mean contact forces on the PF and TF increased by 21% and 10%, respectively, with PCL deficiency in the gait-loading condition.

The mean ligament forces on PFL, LCL, and PT increased by 33.3%, 10.7%, and 71.5%, respectively, with PCL deficiency in the squat-loading condition (Fig. 7b). Unlike the gait-loading condition, more force was exerted on PFL, and, remarkably, it increased on PT.

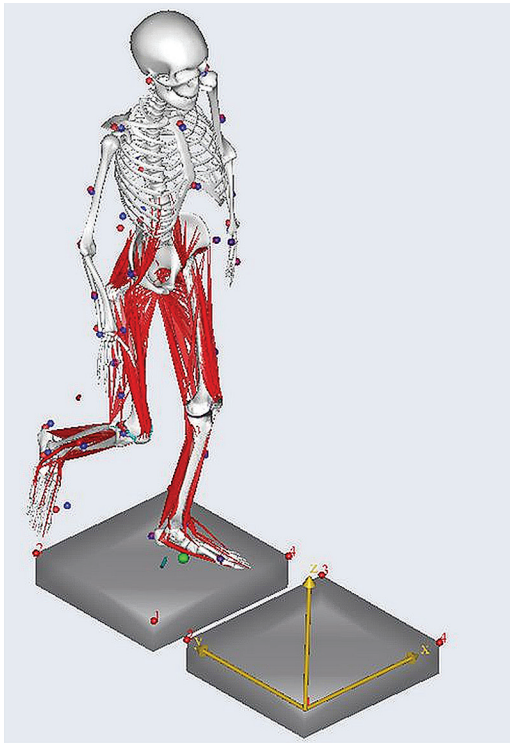


Fig. 3a

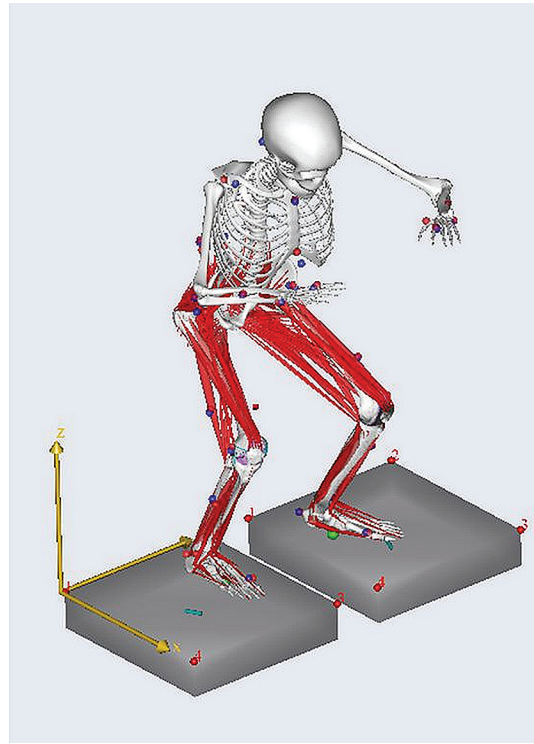


Fig. 3b

Diagram showing subject-specific musculoskeletal model during gait and squat conditions.

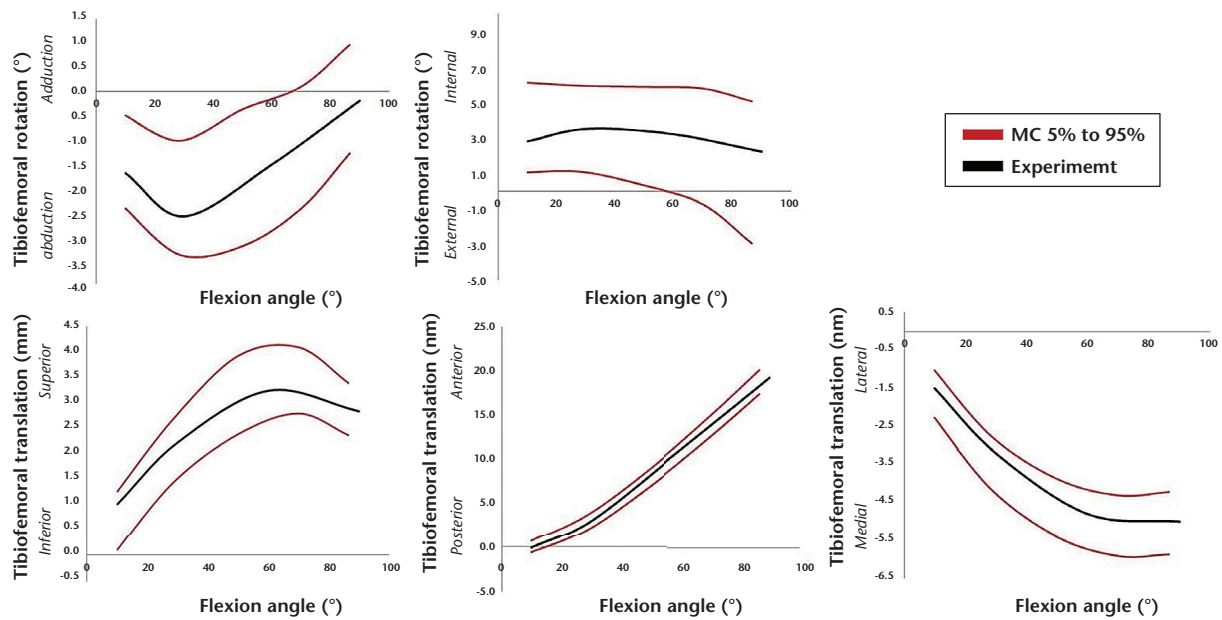


Fig. 4

Graphs showing experimental and Monte Carlo simulation (5% and 95%) for passive flexions from 15 to 90 flexions.

The mean contact forces on TF and PF were 1.95 and 3.78 times body weight, or 1490 N and 2890 N, respectively, with intact model in the squat-loading condition (Fig. 8b). Similar to the gait-loading condition, the contact force on the medial side was greater than that on the lateral side in the squat-loading condition. However,

with PCL deficiency, the mean contact force increased by 25% on the medial side, whereas it decreased by 11.4% on the lateral side during the squat-loading condition. In addition, the mean contact force on the PF joint increased by 72.8%, with PCL deficiency in squatting.

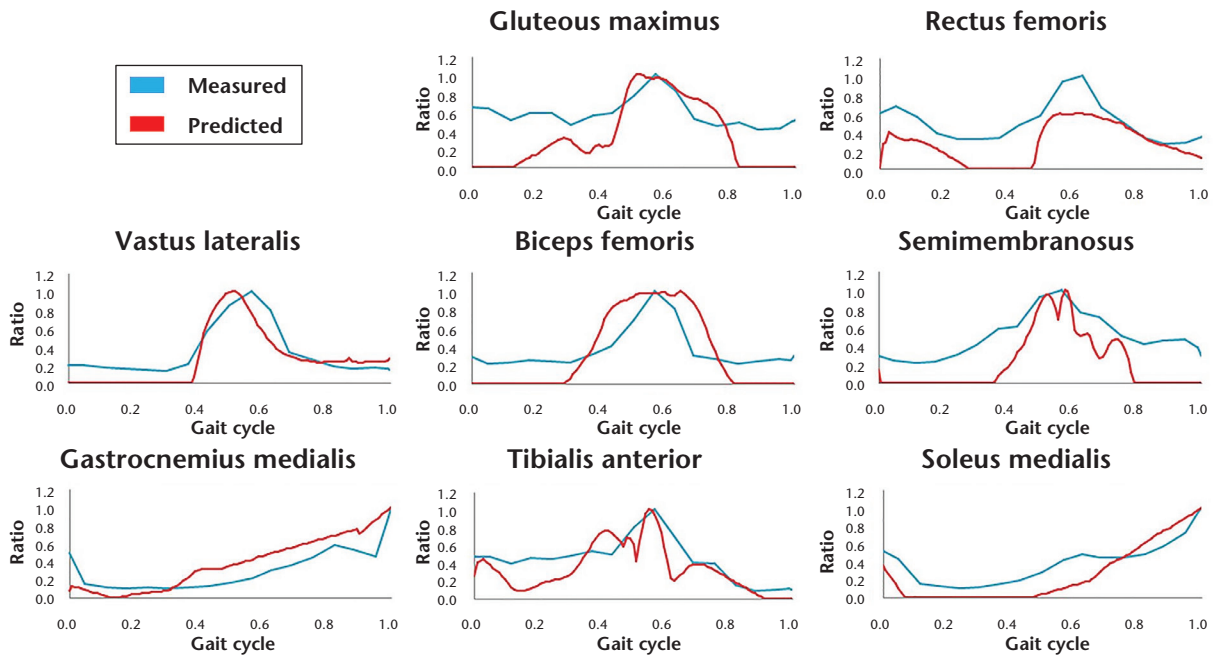


Fig. 5a

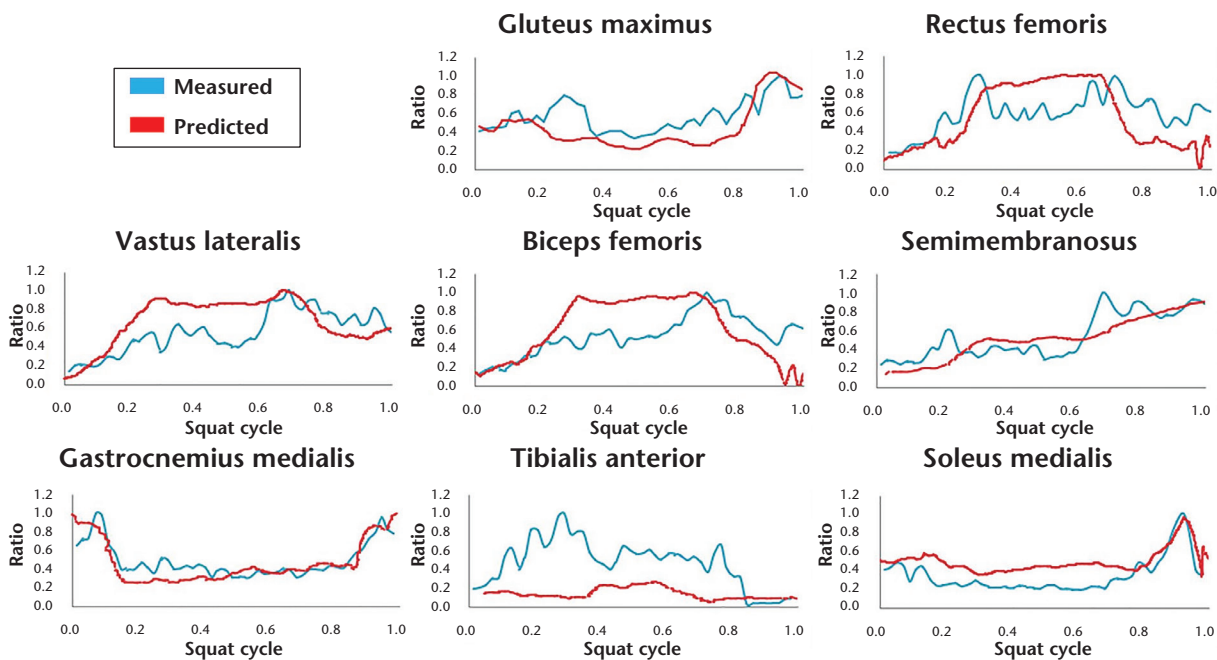


Fig. 5b

Graphs showing comparisons of the muscle activations between experiments and prediction using the subject-specific musculoskeletal model in (a) normal gait and (b) squat conditions.

**Discussion**

The important finding in this study was that the PT is a significant component as a dynamic stabiliser in posterolateral corner structures with PCL deficiency under gait and squat dynamic loading conditions. The dynamics model was developed in this study to evaluate the ligament forces, contact forces on the TF and PF joints, and muscle activation in the knee joint during gait-loading conditions using an MSK model implanted both with and without deficiency of PCL.

Until recently, when the importance of the association between PCL rupture and damage to posterolateral corner structures was recognised, this condition had often been underdiagnosed. There has been a wide variety of treatments for early PCL reconstruction accompanied with a primary repair of the damaged posterolateral corner structure.<sup>55</sup> However, patients often developed chronic injuries due to a delay in diagnosis or presentation, and the optimal treatment method is yet to be established. Posterolateral corner

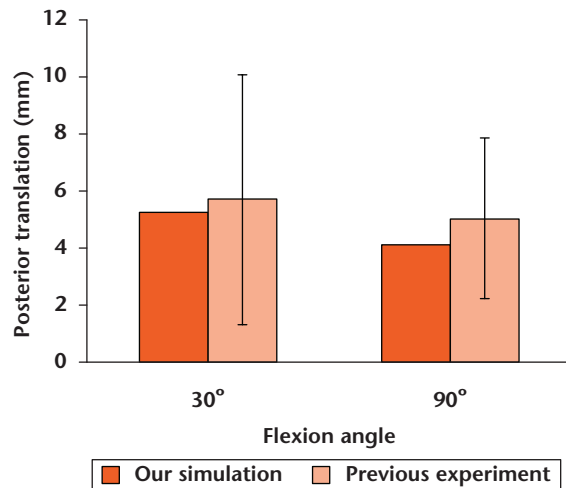


Fig. 6a

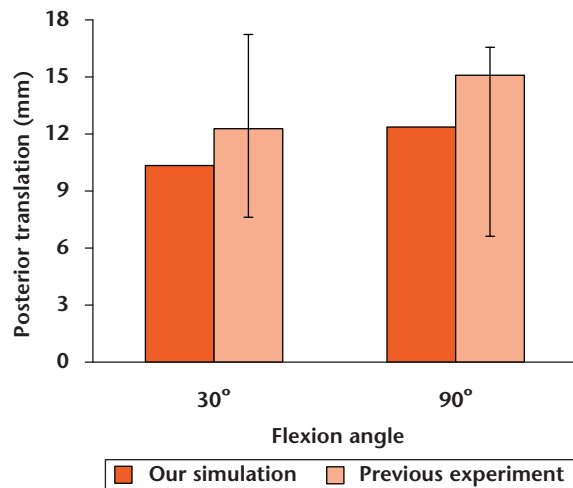


Fig. 6b

Graphs showing a comparison of the posterior tibial translations in the posterior drawer test between (a) intact and (b) posterior cruciate ligament deficient conditions.

structures of the knee comprise many structures that contribute to its static and dynamic stability. The LCL and PFL, both concerned with static components, and the PT, which is concerned with dynamic components, have been described as the major structures of posterolateral corner structures of the knee. Furthermore, the most serious problem in PCL rupture is caused by the posterior displacement of the tibia that is associated with the degeneration of both the medial TF and PF joint compartments. However, in most previous studies, the methodology has been focused on the use of cadavers and medical imaging technology.<sup>16-22</sup>

The PCL is known as the fundamental stabiliser of the knee joint, yet its role in stabilisation is not completely understood.<sup>56</sup> Thus, we introduced and validated an 12-DOF (TF: 6-DOF, PF: 6-DOF) MSK knee model applicable for simulating the force-dependent kinematic method under gait- and squat-loading conditions to evaluate the effects of PCL deficiency.<sup>1-3</sup>

In previous studies, ligaments were considered to be knee joint stabilisers, and four major ligaments, namely ACL, PCL, MCL, and LCL, were conventionally included in the models.<sup>45,57</sup> Most knee joint models have solely included LCL as it is considered to be the primary stabiliser among posterolateral corner structures. However, some sequential sectioning tests have suggested that the PFL and PT also significantly contribute to knee joint stability.<sup>16-19</sup> Recently, a computational knee joint model including the PFL has been introduced.<sup>43,49</sup> However, the PFL is anatomically attached to the PT, and not directly to the femoral bony structure.<sup>9,11,19</sup> Although there is a knee model with the presence of PT-exerted force by point nodes under static loading conditions, it could not substitute the proper structure of PT under dynamic loading conditions.<sup>58</sup>

Therefore, in this study, the PT structure was modelled in as much detail as possible in order to represent

anatomical attachment of the PFL to the PT, not to the fibula, as in a previous study.<sup>49</sup> In addition, the MSK model allows us to represent more realistic daily activity with muscle force interactions which are not under limited flexion, whereas current cadaver or FE studies have not considered robust muscle activation.<sup>16-19,24,26-28</sup> It is a well-acknowledged method in orthopedic biomechanics to evaluate the representative result by using a well-validated computational model.<sup>26-28,43,45</sup>

The PFL did not exert the force, but the LCL and the PT did, with PCL deficiency in the gait-loading condition. The role of the PFL was transformed to PT during gait cycles, and it showed a similar result as a previous study which reported that the LCL is mostly influenced in mid-angle flexion.<sup>16</sup> LaPrade et al<sup>59</sup> reported that there was a significant increase in graft force with a partially-deficient posterolateral corner structure. The graft force became significantly higher with LCL transection during varus loading at both 0° and 30° of knee flexion compared with the identical condition with intact posterolateral corner structures. In addition, coupled loading of varus and internal rotation moments at 0° and 30° of knee flexion increased graft force beyond the condition with varus force alone. However, unlike LCL, the role of the PFL became important in the squat-loading condition. In addition, the ligament force on the LCL was sensitive to the low flexion range. The PT was the most influential component of posterolateral corner structure in both gait- and squat-loading conditions considering its characteristics as a dynamic stabiliser. In addition, the importance of the PT in posterolateral corner structure was validated in a previous study involving cadaveric experiments.<sup>19</sup>

PCL deficiency causes the TF and PF joint degeneration which could aggravate progressive OA.<sup>13,14</sup> It is difficult to establish the mechanism of PF and TF contact force



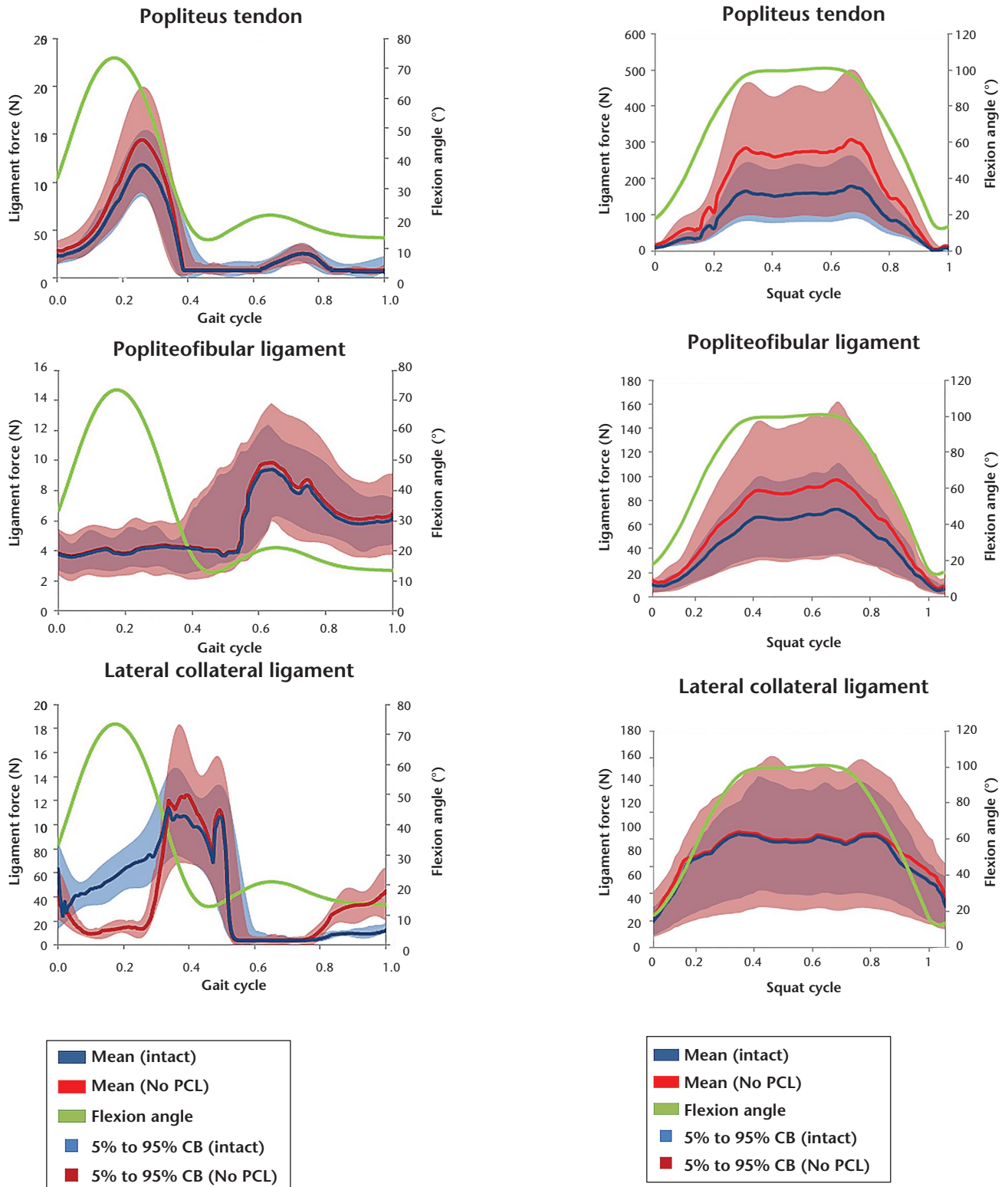


Fig. 7a

Fig. 7b

Graphs showing the forces exerted on the posterolateral corner structure in (a) gait and (b) squat conditions in Monte Carlo simulation (5% and 95%). PCL, posterior cruciate ligament.

after PCL rupture due to the complicated interaction of muscle loading patterns, ligament and capsule deformation, and contact stress distribution on the articular

cartilage in weight-bearing knee *in vivo*.<sup>22</sup> Based on previous *in vivo* measurements at the hip and knee joints, our results provide evidence that the loading conditions

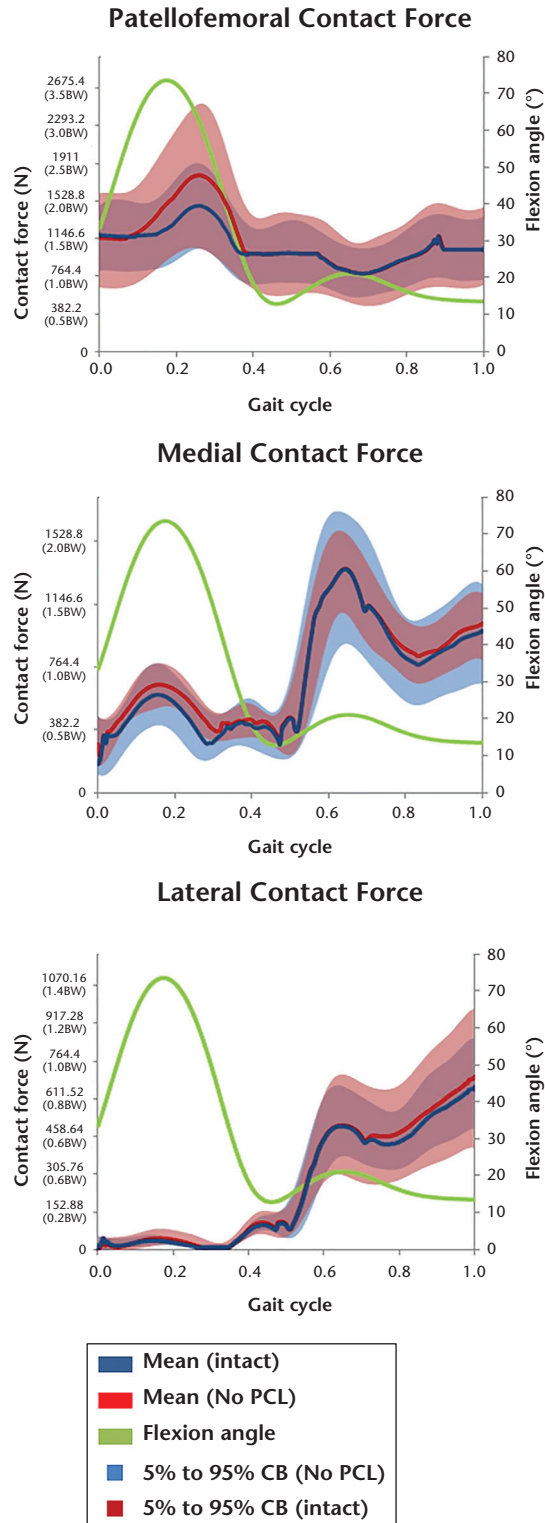


Fig. 8a

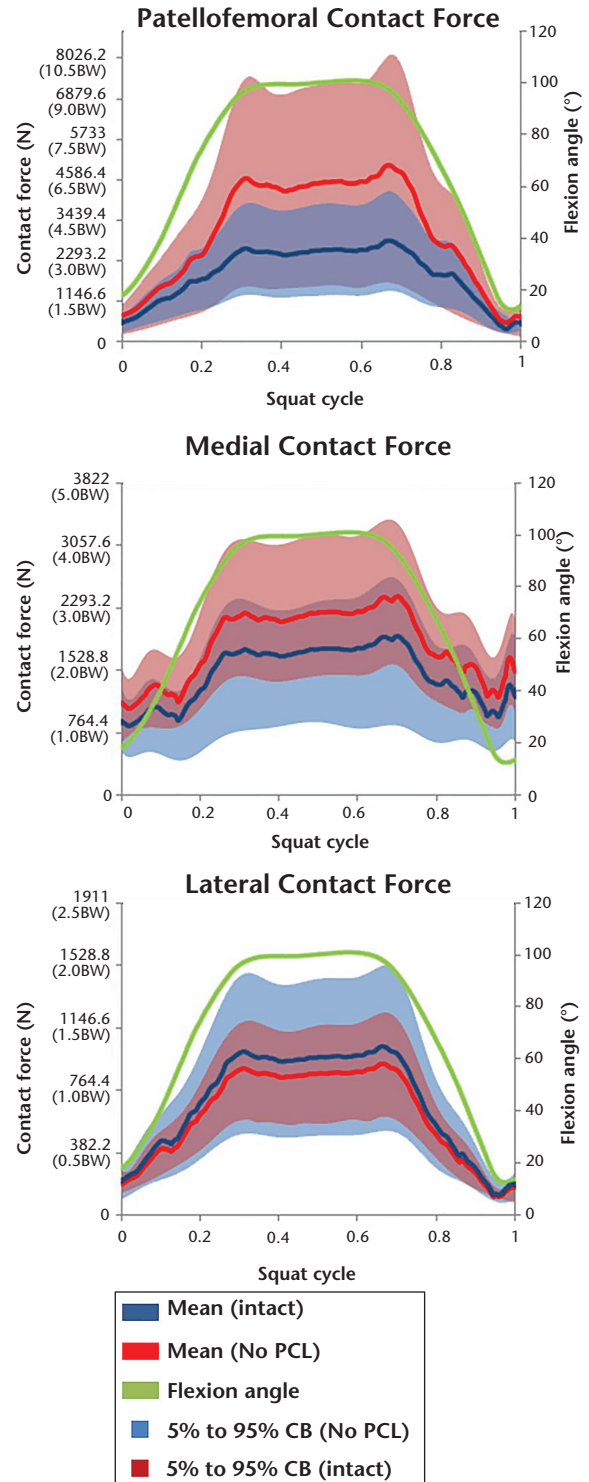


Fig. 8b

Graphs showing the contact force exerted on the tibiofemoral and patellofemoral joint in (a) gait and (b) squat condition in Monte Carlo simulation (5% and 95%). pcl, posterior cruciate ligament.

reach up to three times body weight across the hip and TF and PF joints in daily activities.<sup>60,61</sup>

The contact forces on the TF and PF joints in our model showed good agreement with the results of previous

studies.<sup>43,62,63</sup> The contact forces on the medial side were greater than those on the lateral side in both gait- and squat-loading conditions. Moreover, the ratio of body weight in contact forces in both conditions was

consistent with that in previous studies.<sup>43,62,63</sup> In our model, the contact force on the PF joint became greater than that on the TF joint in high flexion, which showed a similar trend to that observed by Trepczynski et al.<sup>63</sup> The PF joint plays a fundamental role in the knee joint function, particularly in activities associated with high flexion.

To the best of our knowledge, there have been no previous studies that have investigated the contact force on the TF and PF joints in both gait- and squat-loading conditions using a normal knee. There were relatively smaller increases in contact forces on the TF and PF joints in the gait-loading condition. However, in the squat-loading condition, the contact forces on the TF and PF joints increased by 25% and 72.8%, respectively.

An interesting finding was that the contact force on the TF joint increased on the medial side, but decreased on the lateral side. In other words, PCL deficiency may accelerate the degeneration of the TF and PF joints on the medial side due to the increase in contact forces. The contact force on the PF joint particularly increased in high flexion. In our study, there were no differences in either TF or PF joint biomechanics of intact and PCL-deficient knees at 0° and 60° of knee flexion in the gait-loading condition. Therefore, rehabilitation exercises could be safely performed in this flexion range. However, successive deep-squat exercises should be avoided in subjects with PCL deficiency, so as not to alter normal PF cartilage loading excessively. Our data suggest that *in vivo* knee loading can be clearly understood by evaluation of forces on the TF and PF joints.

This study had some limitations. First, only one computational model was developed using data from one subject, although MC simulation was performed to minimize uncertainty in material properties of the ligaments. In addition, the range of values from the subject-specific MSK model was confirmed using data from previous experimental studies; however, the number of subjects could be expanded in future research. Second, ligaments were modified into only two or three bundles. Third, to improve wrapping around the bony structures, wrap objects were included. However, these surfaces were modified to represent simple geometric shapes. Finally, the ground reaction forces were measured directly from feet during gait and squat simulations. Future improvements could be achieved by applying a ground contact model that allows reaction force simulation incorporated with foot-floor interactions.<sup>27</sup>

In conclusion, PCL deficiency primarily influenced the PT among other posterolateral corner structures. The contact forces on the medial side were always greater than those on the lateral side in both gait- and squat-loading conditions. PCL deficiency affects relatively less TF and PF joint contact forces during the gait cycles. However, the contact forces on the TF and PF joints

increased, particularly for the PF joint, with high flexion in the squat-loading condition. In future studies, a larger study sample is required to confirm the present findings.

## References

1. Cain TE, Schwab GH. Performance of an athlete with straight posterior knee instability. *Am J Sports Med* 1981;9:203-208.
2. Hughston JC, Norwood LA Jr. The posterolateral drawer test and external rotational recurvatum test for posterolateral rotatory instability of the knee. *Clin Orthop Relat Res* 1980;82-87.
3. Hughston JC, Bowden JA, Andrews JR, Norwood LA. Acute tears of the posterior cruciate ligament. Results of operative treatment. *J Bone Joint Surg [Am]* 1980;62-A:438-450.
4. Shelbourne KD, Davis TJ, Patel DV. The natural history of acute, isolated, nonoperatively treated posterior cruciate ligament injuries. A prospective study. *Am J Sports Med* 1999;27:276-283.
5. Petrigliano FA, McAllister DR. Isolated posterior cruciate ligament injuries of the knee. *Sports Med Arthrosc* 2006;14:206-212.
6. Schulz MS, Russe K, Weiler A, Eichhorn HJ, Strobel MJ. Epidemiology of posterior cruciate ligament injuries. *Arch Orthop Trauma Surg* 2003;123:186-191.
7. Keller PM, Shelbourne KD, McCarroll JR, Rettig AC. Nonoperatively treated isolated posterior cruciate ligament injuries. *Am J Sports Med* 1993;21:132-136.
8. Parolie JM, Bergfeld JA. Long-term results of nonoperative treatment of isolated posterior cruciate ligament injuries in the athlete. *Am J Sports Med* 1986;14:35-38.
9. Veltri DM, Deng XH, Torzilli PA, Warren RF, Maynard MJ. The role of the cruciate and posterolateral ligaments in stability of the knee. A biomechanical study. *Am J Sports Med* 1995;23:436-443.
10. Hillard-Sembell D, Daniel DM, Stone ML, Dobson BE, Fithian DC. Combined injuries of the anterior cruciate and medial collateral ligaments of the knee. Effect of treatment on stability and function of the joint. *J Bone Joint Surg [Am]* 1996;78-A:169-176.
11. Covey DC. Injuries of the posterolateral corner of the knee. *J Bone Joint Surg [Am]* 2001;83-A:106-118.
12. Levy BA, Dajani KA, Morgan JA, et al. Repair versus reconstruction of the fibular collateral ligament and posterolateral corner in the multiligament-injured knee. *Am J Sports Med* 2010;38:804-809.
13. MacDonald P, Miniaci A, Fowler P, Marks P, Finlay B. A biomechanical analysis of joint contact forces in the posterior cruciate deficient knee. *Knee Surg Sports Traumatol Arthrosc*. 1996;3:252-255.
14. Skyhar MJ, Warren RF, Ortiz GJ, Schwartz E, Otis JC. The effects of sectioning of the posterior cruciate ligament and the posterolateral complex on the articular contact pressures within the knee. *J Bone Joint Surg [Am]* 1993;75:694-699.
15. Boynton MD, Tietjens BR. Long-term followup of the untreated isolated posterior cruciate ligament-deficient knee. *Am J Sports Med* 1996;24:306-310.
16. Gollehon DL, Torzilli PA, Warren RF. The role of the posterolateral and cruciate ligaments in the stability of the human knee. A biomechanical study. *J Bone Joint Surg [Am]* 1987;69-A:233-242.
17. Grood ES, Stowers SF, Noyes FR. Limits of movement in the human knee. Effect of sectioning the posterior cruciate ligament and posterolateral structures. *J Bone Joint Surg [Am]* 1988;70-A:88-97.
18. LaPrade RF, Tso A, Wentorf FA. Force measurements on the fibular collateral ligament, popliteofibular ligament, and popliteus tendon to applied loads. *Am J Sports Med* 2004;32:1695-1701.
19. Chun YM, Kim SJ, Kim HS. Evaluation of the mechanical properties of posterolateral structures and supporting posterolateral instability of the knee. *J Orthop Res* 2008;26:1371-1376.
20. Li G, Gill TJ, DeFrate LE, et al. Biomechanical consequences of PCL deficiency in the knee under simulated muscle loads—an *in vitro* experimental study. *J Orthop Res* 2002;20:887-892.
21. Gill TJ, DeFrate LE, Wang C, et al. The effect of posterior cruciate ligament reconstruction on patellofemoral contact pressures in the knee joint under simulated muscle loads. *Am J Sports Med* 2004;32:109-115.
22. Van de Velde SK, Gill TJ, Li G. Dual fluoroscopic analysis of the posterior cruciate ligament-deficient patellofemoral joint during lunge. *Med Sci Sports Exerc* 2009;41:1198-1205.
23. Weimann A, Schatka I, Herbert M, et al. Reconstruction of the posterior oblique ligament and the posterior cruciate ligament in knees with posteromedial instability. *Arthroscopy* 2012;28:1283-1289.

24. **Liau JJ, Cheng CK, Huang CH, Lo WH.** The effect of malalignment on stresses in polyethylene component of total knee prostheses—a finite element analysis. *Clin Biomech (Bristol, Avon)* 2002;17:140-146.
25. **Werner FW, Ayers DC, Maletsky LP, Rullkoetter PJ.** The effect of valgus/varus malalignment on load distribution in total knee replacements. *J Biomech* 2005;38:349-355.
26. **Colwell CW Jr, Chen PC, D'Lima D.** Extensor malalignment arising from femoral component malrotation in knee arthroplasty: effect of rotating-bearing. *Clin Biomech (Bristol, Avon)* 2011;26:52-57.
27. **Lenhart RL, Kaiser J, Smith CR, Thelen DG.** Prediction and validation of load-dependent behavior of the tibiofemoral and patellofemoral joints during movement. *Ann Biomed Eng* 2015;43:2675-2685.
28. **Shin CS, Chaudhari AM, Andriacchi TP.** The influence of deceleration forces on ACL strain during single-leg landing: a simulation study. *J Biomech* 2007;40:1145-1152.
29. **Thelen DG, Won Choi K, Schmitz AM.** Co-simulation of neuromuscular dynamics and knee mechanics during human walking. *J Biomech Eng* 2014;136:21-33.
30. **Biswas D, Bible JE, Bohan M, et al.** Radiation exposure from musculoskeletal computerized tomographic scans. *J Bone Joint Surg [Am]* 2009;91-A:1882-1889.
31. **Dalmazo J, Elias Júnior J, Brocchi MAC, et al.** Otimização da dose em exames de rotina em tomografia computadorizada: estudo de viabilidade em um hospital universitário. *Radiol Bras* 2010;43:241-248.
32. **van Tiel J, Siebelt M, Waarsing JH, et al.** CT arthrography of the human knee to measure cartilage quality with low radiation dose. *Osteoarthritis Cartilage* 2012;20:678-685.
33. **Good ES, Suntay WJ.** A joint coordinate system for the clinical description of three-dimensional motions: application to the knee. *J Biomech Eng* 1983;105:136-144.
34. **Lloyd DG, Besier TF.** An EMG-driven musculoskeletal model to estimate muscle forces and knee joint moments in vivo. *J Biomech* 2003;36:765-776.
35. **Chen Z, Zhang X, Ardestani MM, et al.** Prediction of in vivo joint mechanics of an artificial knee implant using rigid multi-body dynamics with elastic contacts. *Proc Inst Mech Eng H* 2014;228:564-575.
36. **Klein Horsman MD, Koopman HF, van der Helm FC, Prosé LP, Veeger HE.** Morphological muscle and joint parameters for musculoskeletal modelling of the lower extremity. *Clin Biomech (Bristol, Avon)* 2007;22:239-247.
37. **Forster E.** Predicting muscle forces in the human lower limb during locomotion: VDI-Verlag, 2004.
38. **Ali N, Andersen MS, Rasmussen J, Robertson DG, Rouhi G.** The application of musculoskeletal modeling to investigate gender bias in non-contact ACL injury rate during single-leg landings. *Comput Methods Biomech Biomed Engin* 2014;17:1602-1616.
39. **Kwon OR, Kang KT, Son J, et al.** Biomechanical comparison of fixed- and mobile-bearing for unicompartmental knee arthroplasty using finite element analysis. *J Orthop Res* 2014;32:338-345.
40. **Kim YS, Kang KT, Son J, et al.** Graft extrusion related to the position of allograft in lateral meniscal allograft transplantation: biomechanical comparison between parapatellar and transpatellar approaches using finite element analysis. *Arthroscopy* 2015;31:2380-2391.
41. **Kang KT, Kim SH, Son J, Lee YH, Chun HJ.** Probabilistic Approach for Determining the Material Properties of Meniscal Attachments In Vivo Using Magnetic Resonance Imaging and a Finite Element Model. *J Comput Biol* 2015;22:1097-1107.
42. **Blankevoort L, Huiskes R.** Ligament-bone interaction in a three-dimensional model of the knee. *J Biomech Eng* 1991;113:263-269.
43. **Shelburne KB, Torry MR, Pandey MG.** Contributions of muscles, ligaments, and the ground-reaction force to tibiofemoral joint loading during normal gait. *J Orthop Res* 2006;24:1983-1990.
44. **Marra MA, Vanheule V, Fluit R, et al.** A subject-specific musculoskeletal modeling framework to predict in vivo mechanics of total knee arthroplasty. *J Biomech Eng* 2015;137:020904.
45. **Li G, Gil J, Kanamori A, Woo SL.** A validated three-dimensional computational model of a human knee joint. *J Biomech Eng* 1999;121:657-662.
46. **Fregly BJ, Bei Y, Sylvester ME.** Experimental evaluation of an elastic foundation model to predict contact pressures in knee replacements. *J Biomech* 2003;36:1659-1668.
47. **Terry GC, LaPrade RF.** The biceps femoris muscle complex at the knee. Its anatomy and injury patterns associated with acute anterolateral-anteromedial rotatory instability. *Am J Sports Med* 1996;24:2-8.
48. **Terry GC, LaPrade RF.** The posterolateral aspect of the knee. Anatomy and surgical approach. *Am J Sports Med* 1996;24:732-739.
49. **Baldwin MA, Laz PJ, Stowe JQ, Rullkoetter PJ.** Efficient probabilistic representation of tibiofemoral soft tissue constraint. *Comput Methods Biomech Biomed Engin* 2009;12:651-659.
50. **Harner CD, Vogrin TM, Höher J, Ma CB, Woo SL.** Biomechanical analysis of a posterior cruciate ligament reconstruction. Deficiency of the posterolateral structures as a cause of graft failure. *Am J Sports Med* 2000;28:32-39.
51. **Ma CB, Kanamori A, Vogrin TM, Woo SL, Harner CD.** Measurement of posterior tibial translation in the posterior cruciate ligament-reconstructed knee: significance of the shift in the reference position. *Am J Sports Med* 2003;31:843-848.
52. **Margheritini F, Mauro CS, Rihn JA, et al.** Biomechanical comparison of tibial inlay versus transtibial techniques for posterior cruciate ligament reconstruction: analysis of knee kinematics and graft in situ forces. *Am J Sports Med* 2004;32:587-593.
53. **Sekiya JK, Haemmerle MJ, Stabile KJ, Vogrin TM, Harner CD.** Biomechanical analysis of a combined double-bundle posterior cruciate ligament and posterolateral corner reconstruction. *Am J Sports Med* 2005;33:360-369.
54. **Petersen W, Loerch S, Schanz S, Raschke M, Zantop T.** The role of the posterior oblique ligament in controlling posterior tibial translation in the posterior cruciate ligament-deficient knee. *Am J Sports Med* 2008;36:495-501.
55. **Fanelli GC, Edson CJ.** Posterior cruciate ligament injuries in trauma patients: part II. *Arthroscopy* 1995;11:526-529.
56. **LaPrade CM, Civitarese DM, Rasmussen MT, et al.** Emerging Updates on the Posterior Cruciate Ligament: A Review of the Current Literature. *Am J Sports Med* 2015;43:3077-3092.
57. **Peña E, Calvo B, Martínez MA, Doblaré M.** A three-dimensional finite element analysis of the combined behavior of ligaments and menisci in the healthy human knee joint. *J Biomech* 2006;39:1686-1701.
58. **Kim YH, Purevsuren T, Kim K, Oh KJ.** Contribution of posterolateral corner structures to knee joint translational and rotational stabilities: a computational study. *Proc Inst Mech Eng H* 2013;227:968-975.
59. **LaPrade RF, Resig S, Wentorf F, Lewis JL.** The effects of grade III posterolateral knee complex injuries on anterior cruciate ligament graft force. A biomechanical analysis. *Am J Sports Med* 1999;27:469-475.
60. **Heinlein B, Kutzner I, Graichen F, et al.** ESB Clinical Biomechanics Award 2008: complete data of total knee replacement loading for level walking and stair climbing measured in vivo with a follow-up of 6-10 months. *Clin Biomech (Bristol, Avon)* 2009;24:315-326.
61. **Kutzner I, Heinlein B, Graichen F, et al.** Loading of the knee joint during activities of daily living measured in vivo in five subjects. *J Biomech* 2010;43:2164-2173.
62. **Ramaniraka NA, Terrier A, Theumann N, Siegrist O.** Effects of the posterior cruciate ligament reconstruction on the biomechanics of the knee joint: a finite element analysis. *Clin Biomech (Bristol, Avon)* 2005;20:434-442.
63. **Trepczynski A, Kutzner I, Kornaropoulos E, et al.** Patellofemoral joint contact forces during activities with high knee flexion. *J Orthop Res* 2012;30:408-415.

#### Funding Statement

- None declared

#### Author Contribution

- K-T. Kang: Co-first author, Designing the study, Evaluated the result using computational simulation, Writing the paper
- Y-G. Koh: Co-first author, Designing the study, Data analysis, Writing the paper
- M. Jung: Evaluated the result using computational simulation
- J-H. Nam: Evaluated the result using computational simulation
- J. Son: Developed the 3D model
- Y. H. Lee: Data analysis
- S-J. Kim: Data analysis
- S-H. Kim: Supervisor of study, Data analysis

#### ICMJE Conflicts of Interest

- None declared

© 2017 Kang et al. This is an open-access article distributed under the terms of the Creative Commons Attribution licence (CC-BY-NC), which permits unrestricted use, distribution, and reproduction in any medium, but not for commercial gain, provided the original author and source are credited.